Chimeric β-EF3-α Hemoglobin (Ψ): Energetics of Subunit Interaction and Ligand Binding[†]

L. Kiger,[‡] A. Dumoulin,[‡] S. J. Edelstein,[§] D. J. Abraham,[||] D. Promé,[⊥] C. Poyart,[‡] M. C. Marden,[‡] and J. Pagnier*,[‡]

INSERM U473, 84 rue du Général Leclerc, 94276 Le Kremlin-Bicêtre Cedex, France, Département de Biochimie, Université de Genève, CH-1211, Genève 4, Switzerland, Department of Medical Chemistry, School of Pharmacy, Medical College of Virginia, Virginia Commonwealth University, Richmond, Virginia 23298-0540, and Institut de Pharmacologie et Biologie structurale, CNRS 205 Route de Narbonne 31077 Toulouse, France

Received October 30, 1997; Revised Manuscript Received March 4, 1998

ABSTRACT: Among the numerous strategies to design an oxygen carrier, we outline in this work the engineering of a stable homotetrameric hemoglobin, expressed in *Escherichia coli*. The chimeric globin (Ψ) consists of the first 79 residues of human β globin (corresponding to positions NA1 → EF3) followed by the final 67 residues of human α globin (corresponding to positions EF3 → HC3). The molecular mass for β-EF3-α (Ψ) globin was measured using mass spectrometry to be equal to its theoretical value: 15782 Da. Correct protein folding was assessed by UV/visible and fluorescence spectra. The subunit interaction free energies were estimated by HPLC gel filtration. In the cyanometHb species, the formation of the dimer−tetramer interface is 2 kcal/mol less favorable ($\Delta G = -7$ kcal/mol) than that of Hb A ($\Delta G = -9$ kcal/mol), whereas the dimer−monomer interface is tightly assembled (< −10 kcal/mol) as for the Hb A $\alpha_1\beta_1$ interface. In contrast to Hb A, oxygen binding to Ψ Hb is not cooperative. The free energy for binding four oxygen molecules to a Ψ homotetramer is slightly increased compared to a Hb A heterotetramer (−28 and −27.5 kcal/4 mol of O_2, respectively). The intrinsic O_2 affinity of a Ψ homodimer is 6-fold higher than that of a homotetramer. The linkage scheme between dimer−tetramer subunit assembly and the noncooperative oxygenation of Ψ Hb predicts a stabilization of the tetramer after ligand release. This protein mechanism resembles that of Hb A for which the dimers exhibit a 100-fold higher O_2 affinity relative to deoxy tetramers (which are 10^5 times more stable than oxy tetramers). A potent allosteric effector of Hb A, RSR4, binds to Ψ Hb tetramers, inducing a decrease of the overall O_2 affinity. Since RSR4 interacts specifically with two binding sites of deoxy Hb A, we propose that the chimeric tetramer folding is close to this native structure.

The α and β chains of human hemoglobin associate into different complexes: β_2, β_4, α_2, $\alpha\beta$, and $(\alpha\beta)_2$. The subunit association of α_2 and $\alpha\beta$ complexes is not linked to the oxygenation process (*1*). In contrast, the association of isolated β chains into homotetramer β_4 is more favorable in the oxy state than in the deoxy state by an equivalent energy of 3.4 kcal/mol of tetramer. This is correlated with a lower O_2 affinity for the β monomers compared with the β tetramers. Also, a difference of a few tenths of a kilocalorie per mole has been reported for the last binding step of Hb[1] A tetramers relative to the Hb dimers (*2*), but this quaternary enhancement was not observed by other groups (*3*, *4*).

For Hb A the difference of subunit association free energies between liganded and unliganded states gives rise to its cooperative mechanism upon ligand binding (*5*). At pH 7.4 the quaternary structure of deoxy Hb A is 6.3 kcal/mol more stable compared with oxy Hb A (*2*). This energy represents the difference of O_2 binding free energies between a Hb A tetramer and noncooperative Hb A dimers. The structural basis of the Hb A cooperative mechanism is due to subtle changes which occur at the interfaces between heterogeneous subunits. The quaternary changes observed from the three-dimensional structures of liganded and deoxy Hb correspond to a 15° rotation of one dimer relative to the other (*6*, *7*). While the intradimer interface $\alpha_1\beta_1$ or $\alpha_2\beta_2$ remains essentially rigid, the interdimer "allosteric interface" $\alpha_1\beta_2$ or $\alpha_2\beta_1$ undergoes significant rearrangements of noncovalent interactions which stabilize the Hb quaternary structures. Two regions differ within the allosteric interfaces: the αC−βFG contact, which acts as a "switch region", and the αFG−βC contact which acts as a "flexible region" (*6*). Under typical experimental conditions the T species become predominant after the removal of a second ligand ("switchover point") strengthening the electrostatic and van

[†] This work was supported by INSERM and DGA Contract No. 92-177.

* Corresponding author: INSERM U473, 84 rue du Général Leclerc, 94276 Le Kremlin-Bicêtre Cedex, France. Telephone: (33-1) 46-70-89-89. Fax: (33-1) 46-70-64-46. E-mail: u473@kb.inserm.fr.

[‡] INSERM U473.

[§] Université de Genève.

[||] Virginia Commonwealth University.

[⊥] CNRS 205.

[1] Abbreviations: Bis-Tris, 2-[bis(2-hydroxyethyl)amino]-2-(hydroxymethyl)propane-1,3-diol; DCL Hb, hemoglobin cross-linked between the α chains (Lys99α1 → Lys99α2) by bis(3,5-dibromosalicyl) fumarate; IHP, inositol hexakisphosphate; Hp, haptoglobin; Hb, hemoglobin; MetHb, methemoglobin; Mb, myoglobin; RSR4, 2-[4-[[(3,5-dichloroanilino)carbonyl]methyl]phenoxy]-2-methylpropionic acid; Ψ Hb, chimeric β-EF3-α Hb (see definition in Abstract).

S0006-2960(97)02689-5 CCC: $15.00
Published on Web 05/02/1998

der Waals contacts located at the allosteric interface compared with the R species (*2*). Unfavorable interactions also seem to be of importance in the decrease of stability for the $\alpha_1\beta_2$ and $\alpha_2\beta_1$ interfaces during the T → R transition (*8*). Generally, the contacts localized at the allosteric interface are so highly evolved that a mutation among one of the constitutive amino acids is likely to affect the cooperative free energy (*9*).

The two-state model (*10*) predicts a shift of the R ⇌ T allosteric equilibrium of Hb A for each O_2 molecule bound by a constant factor; in standard conditions this factor is about 100. Within this context, the functional inequivalencies, not considered by this simple model, between the α and β subunits and between the doubly liganded species (i.e., asymmetric versus symmetric hybrid; refs *11*−*17*) are minor perturbations compared to the shift in allosteric equilibrium per ligand. In the concerted model each Hb A intermediate species is in equilibrium between the quaternary R and T structures. The quaternary constraints generated during the allosteric transition from R to T give rise to the tertiary constraints that lower the O_2 affinity of the four subunit binding sites (*5*).

Chimeric protein construction appears to be of paramount importance for protein engineering. With mutagenesis methods it is possible to create de novo proteins which consist of domains from two different proteins, intra- or interspecies. Those proteins take advantage of structural and/or functional properties of their various components (*18*−*21*). The goal of our work was to produce a stable recombinant homotetramer from a chimeric globin formed by half the primary sequences of the heterologous α and β chains. A chimera generally refers to a hybrid made of parts from distinct origins. Thus the in vitro mixing of human alpha chains and beta chains of a different species can form chimeric tetramers and vice versa. More recently, interspecies hybrids were obtained in vivo in transgenic swine expressing human Hb (*22*). An individual subunit can also be chimeric when composed of fragments of existing chains; this occurs naturally for Lepore Hbs where there is a fusion of the δ and β genes (*23*). Such chimeric chains still associate with normal α chains to form heterotetramers. The Ψ chains of this study are of this latter type of chimera, with the additional interest of forming a homotetramer.

A first chimera Hb was produced in our laboratory with a cleavage region located in the distal heme pocket region at the E17 residue (*24*). The electrophoretic migration pattern indicated that this chimera protein was heterogeneous, which prevented a detailed study of the subunit aggregation equilibria. In this work the C-terminal sequence of the β chain after the EF3 residue was replaced by the corresponding C-terminal sequence of the α chain. The rationale of both designs was to choose a cleavage region located in a flexible region of the protein and to preserve to a large extent the residues involved in the allosteric interface of Hb A and/or in the interactions with the heme moiety. Since the allosteric interface cohesion requires several contacts between two main globin domains (the FG corner and the C helix of the α and β subunits), the possible cleavage region of our chimera globin design was necessarily located in the heme pocket formed by the E and F helices (see Figure 1 from ref *24*). Consequently, a tetrameric Ψ Hb form might retain at least partially the homotropic and/or the heterotropic effects that characterize the interactions of Hb A with ligands and effectors.

We compared the amino acids involved in the inter- and intradimer interfaces of Hb A and β_4 tetramers with those present in the primary sequence of Ψ Hb. Schaad et al. (*25*) have determined the residues contributing to the different interfaces of Hb A and β_4 tetramers using computer-based model building and energy minimization. In the interdimer interfaces 60% and 45% of the contacts for Hb A and β_4, respectively, could be preserved in the Ψ tetramer compared to only 25% in the intradimer interfaces for both structures. Those observations did not allow us to anticipate a preferential association mechanism of the Ψ subunits. The intradimer interface in the homotetramer β_4 is much less stable than that of the $\alpha\beta$ dimer (*26*, *27*). Consequently, there are relatively few β_2 dimers but appreciable quantities of β monomers in equilibrium with β_4 tetramers in the micromolar range of heme concentration. Under similar conditions, Hb A is in equilibrium between tetramers and dimers; significant amounts of α and β monomers will be detected only in the picomolar range. One might assume that the chimeric tetramers closely resemble β_4 tetramers because the globin possesses the D helix sequence that is absent in the α subunit. However, Komiyama et al. (*28*) have shown that addition of a D helix to the α chain, or removal from the β chain, does not change the allosteric mechanism of the $\alpha_2\beta_2$ tetramer.

To elucidate the structural and functional properties of the chimeric Ψ Hb, we used several biochemical and biophysical methods. We assessed the purity of the recombinant Hb and showed the absence of any protein contamination and posttranslational modifications. By measuring UV/visible and fluorescence spectra, we detected a satisfactory refolding of the chimeric globin and no heme loss. Time-resolved and static spectrophotometries were exploited to determine the O_2 and CO binding properties of the Ψ Hb in the absence or presence of potent allosteric effectors. The subunit assembly reaction was analyzed by gel filtration. The Ψ Hb exhibits an O_2 affinity intermediate to the R and T states of Hb A; we therefore discuss the perspectives of engineering such recombinant homotetramers as O_2 carriers.

MATERIALS AND METHODS

Expression and Purification of the Hb Variant Produced in E coli. The DNA fragments coding for the NA1-EF3 β globin and the EF3-HC3 α globin were amplified starting from plasmids containing the β cDNA and the α cDNA, respectively. The two primers corresponding to the junction area (EF3 region) were designed to be complementary to each other and orientated in the opposite direction. The chimeric β/α cDNA construction was achieved by a global PCR after mixing the two purified fragments resulting from the initial amplification reactions, the complementarity in the EF3 region allowing the two fragments to fuse. The β/α sequence was digested using appropriate restriction enzymes and inserted into the expression vector pATPrTet (*29*). This vector directs the synthesis of the chimeric globin fused to the first 31 amino acids of the λ protein cII with the sequence Ile-Glu-Gly-Arg in between. The expression is controlled by a strong heat-regulated λ Pr promotor. The pATPrcIIFX chimera plasmid was transformed into *E. coli* strain CAG

1139. The exponential growth phase was initiated at 30 °C in a fermentor containing 15 L of culture medium. The fusion protein production was initiated by switching the temperature to 42 °C, which inactivates the temperature-sensitive repressor cI857. The cells were harvested after 3−4 h incubation, and the fusion protein was extracted, purified, and cleaved with factor Xa to produce the Ψ globin (*30*). The Ψ globin was reconstituted with hemin-CN and purified by successive ion-exchange chromatographies. Two heminized fractions were collected at the last step of purification; each of these migrated as a single distinct component on SDS−polyacrylamide gel electrophoresis. The band close to the human β chain was attributed to the Ψ globin, whereas the band closer to the fusion protein marker was attributed to a heminized fusion protein including the Ψ globin sequence. An additional isoelectrofocusing (IEF) of cyanometHb derivatives was performed in polyacrylamide gel (Pharmacia Biotech) along a gradient from pH 6.5 to 8.5 with the LKB system, to check the homogeneity of the heminized Ψ globin preparation. Finally, the chimeric cyanometHb solution equilibrated under 1 atm of CO was reduced with sodium dithionite, stripped onto a G25 Sephadex column, and stored in liquid nitrogen until use.

Hb A was purified from the blood of healthy donors, stripped of organophosphates, and stored in liquid nitrogen. Horse Mb type III (Sigma Chemical Co.) was equilibrated under CO and then reduced with sodium dithionite. Excess dithionite and side products were removed by passing the sample through a Sephadex G25 column at 5 °C. Mb samples, as well as other CO samples, were decarboxylated under light exposure at 0 °C inside a tonometer flushed with pure O_2.

Human α and β chains were split from Hb A upon reaction with *p*-mercuribenzoate following the procedure of Winterhalter and Colisimo (*31*) with some modifications. PMB chains were then separated according to the method of Bucci and Fronticelli (*32*). The SH groups were regenerated with 2-mercaptoethanol, and the purity of the α and β preparations was verified by IEF as described above.

Human haptoglobin (Hp), a glycoprotein of the serum, binds two hemoglobin dimers. There are two autosomal alleles which encode Hp 1 and 2, and thus three different genetic groups can be observed: 1−1, 1−2, and 2−2. Because interactions between Hb and Hp have been extensively studied with Hp type 1−1, the experiments reported in this work were fulfilled with this Hp phenotype purchased from Sigma.

Gel Filtration Chromatography. Protein samples were passed through a Superose 12 PC 3.2/30 column using a Pharmacia HPLC system. The column was loaded with 20 μL of a protein using a Hamilton syringe and eluted with 50 mM Bis-Tris, 100 mM NaCl, 1 mM EDTA, and 0.1 mM KCN, pH 7.3, at 21 °C. The flow rate was constant and equal to 0.04 mL/min. The dilution factor for each elution profile was estimated by the ratio of the width at half-height (converted into milliliters) to the sample volume. From the average of more than 20 experiments the dilution factor was found to be 2.5 ± 0.2. Included (V_i) and excluded (V_0) volumes were measured by using a 10% acetone solution in distilled water and human immunoglobulins from Biotransfusion, respectively. The elution volume of a protein sample (V_e) corresponds to the elution profile peak. The absorbance of the eluent in the UV/visible domain was monitored simultaneously at 280, 422, and 540 nm.

From the column characteristics, the weight-averaged partition coefficient, $\overline{\sigma_w}$, is given by the relationship

$$\overline{\sigma_w} = \frac{V_e - V_0}{V_i}$$

For an $\alpha_2\beta_2$ Hb tetramer this coefficient depends on the fractions of dimers (f_D) and tetramers (f_T) and their respective partition coefficients, σ_D and σ_T, following the relationship

$$\overline{\sigma_w} = f_D\sigma_D + f_T\sigma_T$$

Finally, dimer and tetramer fractions are related to the protein concentration in heme units (P_t) and the equilibrium constant ($^4K_2$) of the dimer−tetramer autoassociation by the following relationship:

$$f_D = \frac{-1 + \sqrt{1 + 4(^4K_2P_t)}}{2(^4K_2P_t)} \qquad f_T = 1 - f_D$$

The elution volume of a Hb tetramer was determined with a 2 μM solution of cross-linked DCL Hb (Baxter Healthcare; *33*) and the elution volume of a Hb dimer with a 2 μM solution of the natural variant Hb Rothschild Trp β37 → Arg, which is entirely dissociated into dimers at low Hb concentration (*9*). The elution volume of a Hb monomer was determined with a 2 μM solution of α chain. Partition coefficients σ_D and σ_T estimated from these values were added to the subunit association isotherm of Hb A to constrain the end-point simulations.

Electrospray Mass Spectrometry. An electrospray dedicated Fisons TRIO 2000 instrument (Micromass VG-Biotech, Manchester, U.K.) was used for mass spectrometry. Samples were dissolved in an acetonitrile/water/formic acid mixture (50:49:2) at a concentration of 10 pmol/μL. Ten microliters was injected into the 10 μL/min flow of the same solvent. The capillary voltage was 4 kV. The cone-to-skimmer potential was 50 V. Normal β chain was used for external calibration. The VG MaxEnt program was then used to process the spectrum, thus improving the accuracy of the molecular mass determination and the resolution of the protein spectrum. The accuracy was estimated as better than 2 Da. The crude spectrum was constituted from a series of peaks which correspond to the protein with different protonation states. Computer calculations transformed the mass over charge scale into a true mass scale showing the calculated molecular weight of the proteins.

Absorption Spectra. Uv/visible static absorption spectra of Hb A and Ψ Hb solutions in a quartz cuvette of 4 mm optical path length were recorded with an SLM-Aminco (DW2000) spectrophotometer. Oxy ferrous spectra were measured under 1 O_2 atm in the presence of the reductive enzyme system reported by Hayashi et al. (*34*). Deoxy ferrous spectra were measured after flushing thoroughly the samples under argon followed by addition of a slight excess of sodium dithionite to keep the hemes totally reduced. From the deoxy solutions CO spectra were recorded after equilibration under CO gas. Cyanomet species was used to determine the heme concentration, taking an ϵ value of 11

mM^{-1} cm^{-1} at 540 nm (*35*, *36*). Since enzymes and coenzymes, sodium dithionite, and potassium ferricyanide absorb in the UV domain, their control spectra were subtracted from the sample spectra.

Fluorescence Spectra. Fluorescence spectra were recorded for protein concentrations (on a heme basis) of 3 μM using an SLM 8000 spectrofluorometer. CyanometHb samples were equilibrated in 20 mM sodium phosphate, pH 7.0, at room temperature. At 280 nm excitation, the intensity of fluorescence emission between 300 and 400 nm is a sensitive test of the quality of the protein refolding for reconstituted hemoproteins since the tyrosine and tryptophan residues are normally highly quenched by the hemes. The comparison of fluorescence emission spectra between Hb A (6 tryptophans per tetramer) and Ψ Hb (8 tryptophans per tetramer) is valid because tryptophan residues are located at the same positions in both proteins: A12 and C3 in the β and Ψ chains, A12 in the α chains of Hb A. Although we cannot assume that tryptophan side chains of Ψ Hb are in the same orientation as in Hb A with respect to the hemes, a large increase of fluorescence intensity would indicate either a loss of heme or a partial unfolding. For example, an increase of fluorescence intensity of 50% is expected if 1% of the globin content is unquenched.

Autoxidation Studies. The absorption spectra during autoxidation were measured between 350 and 700 nm every 30 min during 12 h with an SLM-Amicon DW2000 spectrophotometer. Protein samples were equilibrated under 1 atm of O_2 in 50 mM Bis-Tris buffer and 100 mM NaCl, pH 7.0, at 37 °C. The fully oxidized spectrum was obtained after a slight addition of potassium ferricyanide. The contribution of this compound to the absorbance was subtracted from the blank. Protein concentrations were determined at 540 nm after addition of dry KCN as described above under Absorption Spectra.

At each time of measurement the fraction of remaining ferrous heme was determined by simulating the whole spectrum as a linear combination of the fully oxygenated and oxidized spectra. The decrease of the ferrous heme fraction was fitted as a first-order reaction.

Oxygen Binding Curves. Oxygen equilibrium binding curves were recorded with a continuous method by means of a Hemox analyzer (TCS). The stability of the optical detection and the efficiency of the gas diffusion to solution at equilibrium were confirmed by recording virtually identical deoxygenation and reoxygenation O_2 isotherms for a Hb A sample. A reductive enzyme system (*34*) was used to prevent metHb formation (*2*). OxyHb spectra were measured after the deoxygenation process, showing no apparent metHb formation. The O_2 binding isotherms of Hb A were analyzed with a nonlinear least-squares fitting procedure (*37*). From these isotherms we obtained the median partial pressures P_{med}, the partial pressures at half-saturation, P_{50}, and the Hill coefficient, n (*37*). The Hill coefficient is calculated as follows:

$$n = \frac{d\log(\bar{Y}/(1-\bar{Y}))}{d\log(PO_2)}$$

The O_2 isotherms of Ψ Hb were fitted using the partition functions for dimers and tetramers (*2*, *38*). According to the nomenclature used by Ackers and colleagues:

$$\bar{Y} = \frac{Z'_2 + Z'_4\{\sqrt{(Z_2)^2 + 4({}^0K_2Z_4P_t)} - Z_2\}/(4Z_4)}{Z_2 + \sqrt{(Z_2)^2 + 4({}^0K_2Z_4P_t)}}$$

where

$$Z_2 = 1 + 2\beta_D[O_2] + \beta_D{}^2[O_2]^2$$

$$Z'_2 = 2\beta_D[O_2] + 2\beta_D{}^2[O_2]^2$$

$$Z_4 = 1 + 4\beta_T[O_2] + 6\beta_T{}^2[O_2]^2 + 4\beta_T{}^3[O_2]^3 + \beta_T{}^4[O_2]^4$$

$$Z'_4 = 4\beta_T[O_2] + 12\beta_T{}^2[O_2]^2 + 12\beta_T{}^3[O_2]^3 + 4\beta_T{}^4[O_2]^4$$

P_t is the protein concentration in heme units, $[O_2]$ is the ligand activity, ${}^0K_2$ is the dimer−tetramer equilibrium constant in the deoxy state, and β_D and β_T are the intrinsic O_2 affinities for dimers and tetramers. β_D and β_T were constrained to be equal for each step of ligation due to the absence of cooperativity upon ligand binding. The values of β_D and β_T were estimated by the flash photolysis experiments described in the following section. The fits of O_2 isotherms were obtained when the value of ${}^0K_2$ was floated.

O_2 and CO Recombination after Flash Photolysis. O_2 and CO bimolecular recombination rates (k_{on}) were measured after flash photolysis with a 10-ns YAG laser pulse delivering 160 mJ at 532 nm (Quantel). Samples were equilibrated respectively under air or 1 atm of CO in 1 mm or 4 mm optical cuvettes with a detection wavelength at 436 nm. A typical kinetic curve was obtained after an average of 10 measurements. A reducing enzyme system (*34*) was added to the oxygenated samples to eliminate the residual methemoglobin fraction. Sodium dithionite solution was added to a final concentration of 0.5 mM under CO atmosphere to prevent O_2 contamination and to keep the Hb samples fully reduced. The best simulations of normalized bimolecular kinetics were obtained with one or two exponential terms.

The O_2 off-rate value ($k_{off}{}^{O_2}$) of Ψ Hb in the dimeric or tetrameric forms were measured by the O_2/CO replacement reaction after flash photolysis. Several mixtures of O_2 and CO gas were adjusted: 145:50, 140:100, and 130:150 mmHg. Under these conditions the proportion of free binding hemes is negligible, and consequently a steady state is established in which the deoxy Hb concentration is constant. The differencial equations which give the rates of consumption/formation for deoxygenated, oxygenated, and carboxylated species can be combined to obtain an irreversible first-order reaction because the CO dissociation is slow (*39*). The replacement phase was analyzed versus the protein concentration to extract the O_2 off-rates for Ψ Hb dimers and tetramers (dimer and tetramer fractions were estimated from the value of ${}^4K_2$).

O_2 and CO Dissociation Kinetics. Kinetics of O_2 dissociation for other proteins were measured with a stopped-flow spectrophotometer (Biologic) by mixing oxy samples with a sodium dithionite solution to consume free O_2 molecules during the apparatus dead time (≈3 ms). The concentration of sodium dithionite was 10 mM after mixing, which corresponds approximately to a 100-fold excess relative to the O_2 concentration. No side reaction from

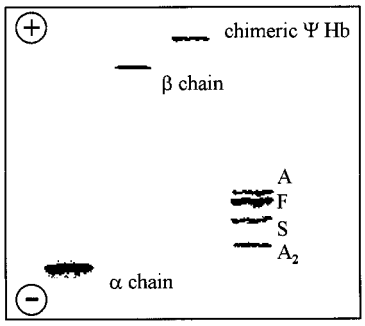

FIGURE 1: Isoelectric focusing in polyacrylamide gel of Ψ Hb (see Materials and Methods) compared with isolated α and β chains (β_4), Hb A ($(\alpha\beta)_2$), and the Hb natural variants Hb F, S, and A_2. The chimeric Hb focuses at a position close to that of the homotetramer β_4.

dithionite and O_2 products was observed during the fast kinetics of O_2 dissociation, and the reaction amplitude was in agreement with that estimated from the oxy and deoxy static spectra. The wavelengths of detection were near the Soret peaks of the oxy and deoxy spectra, 415 and 430 nm, respectively. The normalized traces of opposite sign at these two wavelengths gave identical results.

Kinetics of CO dissociation were measured after dilution of CO samples into a 6 mM potassium ferricyanide solution. The changes of absorbance were monitored with a dual-beam mode at 700 and 420 nm using an SLM-Aminco DW2000 spectrophotometer. For these experiments a quartz cuvette of 2 mm optical path length was used.

All the kinetics were simulated with a standard exponential analysis as described in the previous section. Data simulations and standard errors were carried out using the nonlinear least-squares routine of the software program Scientist.

Experimental Conditions. When the experimental conditions are not mentioned, the experiments were performed in 50 mM Bis-Tris, 100 mM NaCl, and 1 mM EDTA, pH 7.2, at 25 °C. The buffer was filtered on a 0.22 μM filter (Millipore). Sodium dithionite solution was prepared daily in a deoxygenated buffer. The effector RSR4 was synthesized as described (*40*), and 10 mM stock solution, pH 7.0, was used for the experiments; the final concentration of effector was 0.5 mM. O_2, CO, and argon gases were from Air Liquide Co. (Paris, France). O_2 and Ar were humidified during equilibration of the samples. Partial gas pressures were converted to molarities using Henry's law constants 1.6×10^{-6} and 1.2×10^{-6} M $Torr^{-1}$ for O_2 and CO, respectively. The O_2 partial pressure was obtained by subtracting the vapor pressure (24 mmHg at 25 °C) from the barometric pressure.

RESULTS

Purity of Ψ Hb Preparation. Isoelectrofocusing of Ψ Hb showed a single heminized band migrating to a lower isoelectric pH value than that of a human β chain (Figure 1) (gel filtration experiments described in the following sections confirmed the absence of nonheminized protein contamination from *E. coli*). The p*I* of β chains is close to 5.7 ± 0.1, while for comparison the p*I*'s of Hb A, Hb F, Hb S, and Hb A_2 are 6.95, 7.05, 7.2, and 7.4, respectively, and that for α chains is 7.8. The p*I* of Ψ Hb was calculated to be 5.6 ± 0.1. As the quaternary structure of Ψ Hb is unknown, it is hypothetical to predict its p*I* on the basis of the primary sequence. However, a comparison among the p*I* values reported above is consistent with their relative amounts of positively and negatively charged amino acids.

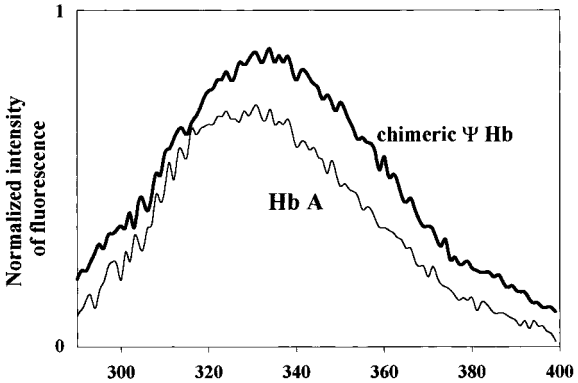

FIGURE 2: Fluorescence emission spectra of cyanometHb Ψ Hb and Hb A (3 μM in heme). Excitation wavelength was 280 nm. The weak intensity of the tryptophan fluorescence in both proteins is due to the fluorescence quenching by the heme moiety. This indicates correct protein folding and no heme loss for Ψ Hb. The slight increase of fluorescence intensity for Ψ Hb may be due to the presence of eight tryptophans per tetramer compared to six in Hb A.

Electrospray Mass Spectroscopy (ESMS). EMS is a powerful technique to measure accurately the molecular mass of molecules (*41*). The analysis of the primary sequence of recombinant Ψ Hb by standard biochemical methods is time-consuming, requires more material, and does not eliminate the risk of any undetected post-transductional modifications from *E. coli*. The measured molecular mass was 15782.9 Da, whereas the expected molecular mass is 15781.9 Da. This result validates unambiguously the Ψ Hb primary sequence.

Fluorescence Spectra. Fluorescence emission is very sensitive to the folding of hemoproteins since tryptophan fluorescence is highly quenched by the heme moiety. In the case of Hb A, the addition of heme to an apoglobin solution will decrease the fluorescence intensity by a factor of 50 (*42*). The fluorescence has been used as a sensitive probe to measure the unfolding of several hemoproteins submitted to high pressures (*43*). The emission of fluorescence is shown for Ψ Hb and Hb A in Figure 2. The intensity of fluorescence of Ψ Hb was similar to that of Hb A and confirmed a satisfactory folding of the chimeric Hb and heme binding to the globin.

UV and Visible Spectra. We measured UV and visible optical spectra of oxy, deoxy, CO, and oxidized forms for Ψ Hb and Hb A. The extinction coefficients and peak positions are summarized in Table 1. No significant differences between Ψ Hb and Hb A derivatives were observed except for a 17% decrease of the Soret band of the deoxy ferro-compounds. The difference spectrum of deoxy Soret bands is shown in the inset of Figure 3. This difference has already been interpreted as a T deoxy minus R deoxy spectrum on the basis of studies with NES-des-Arg-hemoglobin. This variant is a chemically modified Hb in which the α C-terminal residue, involved in a salt bridge formation that stabilizes the T structure, is removed by enzymatic reaction. In addition, the β F9 Cys is reacted with *N*-ethylmaleimide, which disrupts the salt bridges formed

Table 1: Near-UV/Visible Extinction Coefficients of Ψ Chimeric Hb and Hb A Peaks

oxygenated ferro compound				carboxylated ferro compound				deoxygenated ferro compound				ferri compound			
Ψ Hb		Hb A		Ψ Hb		Hb A		Ψ Hb		Hb A		Ψ Hb		Hb A	
λ (nm)	ϵ	λ (nm)	ϵ	λ (nm)	ϵ	λ (nm)	ϵ	λ (nm)	ϵ	λ (nm)	ϵ	λ (nm)	ϵ	λ (nm)	ϵ
414	135.4	415	128.4	420	191.4	420	191.0	430	114.2	430	138.1	406	154.6	406	157.6
542	14.7	541	14.2	539	13.9	539	13.7	557	12.3	555	12.9	500	8.9	500	9.2
576	14.8	576	14.9	568	13.9	569	13.9					630	3.3	630	3.4

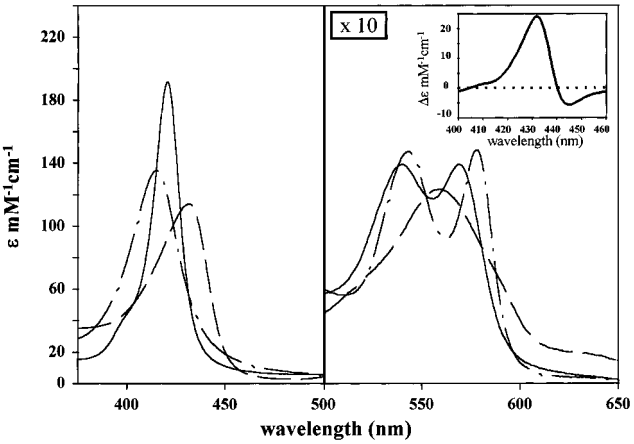

FIGURE 3: Deoxy (long dash), oxy (dash−dot), and CO (solid line) UV and visible absorption spectra of Ψ Hb. The α and β peaks are magnified 10-fold. The inset shows the difference spectrum between deoxy Hb A and deoxy Ψ Hb, which is similar to a T deoxy minus R deoxy spectrum of Hb A.

by the β C-terminal HC3 His (*44*, *45*). Its deoxy form remains in an R-like structure but is able to switch to a T-like structure upon binding of the strong allosteric effector IHP. The difference spectrum of deoxy NES-des-Arg-hemoglobin with and without IHP (*44*) exhibits a similar shape and intensity to the difference spectrum between Ψ Hb and Hb A. However, the spectral difference of NES-des-Arg-hemoglobin could be slightly underestimated because the fraction of dimer is significant at the 10 μM heme concentration used by the authors (*9*). The same spectral difference has been observed after mixing equimolar solutions of deoxy α and β chains which autoassociate into Hb A deoxy tetramer (*39*). This spectral change for the aggregation of isolated chains is essentially due to the α chain contribution (*46*).

We further characterized the chimera by measuring the near-infrared band III of Ψ globin. The band III observed in deoxy ferro-compounds has been assigned to charge transfer between π-porphyrin and iron electrons (*47*). Band III correlates well with the bimolecular rate of CO association (*48*) and with the stretch frequency of the Fe−His (F8) bond. The Gaussian shape and position (762 nm) of the band III for EF3 β/α globin and α chain were similar (data not shown), suggesting similar proximal constraints exerted by the heme pocket on the heme moiety, via the Fe−His (F8) bond. This is consistent with the sequence of Ψ globin, which is formed by the F and G helices of the α globin. The band III position is also sensitive to the polarity of the distal side of the heme (*48*). A red-shift of band III to around 770 nm would have indicated the lack of polar residues in the vicinity of the heme. Since the E7 position is occupied by a distal histidine, in both the α and β chains, the acceptance of a water molecule in the distal heme pocket of the metHb, as revealed by the characteristic 406-nm position of the Soret, is not surprising.

Table 2: Free Energies of Subunit Assembly

equilibrium	species	state of ligation	$\Delta G_{assembly}$ (kcal/mol)
tetramer ↔ dimer[a]	Ψ Hb	cyano-metHb	-7.1 ± 0.2
tetramer ↔ dimer[a]	Ψ Hb	deoxygenated	-11.1 ± 0.9
dimer ↔ monomer[a]	Ψ Hb	cyano-metHb	<-10
tetramer ↔ dimer[a]	Hb A	cyano-metHb	-8.9 ± 0.1
dimer ↔ monomer[b]	Hb A	carboxylated	-17
tetramer ↔ dimer[c]	Hb A	oxygenated	-8.0 ± 0.1
tetramer ↔ dimer[c]	Hb A	deoxygenated	-14.3 ± 0.2
tetramer ↔ dimer[d]	β^A chain	carboxylated	-8.6 ± 0.2
dimer ↔ monomer[d]	β^A chain	carboxylated	-6.5 ± 0.3
tetramer ↔ monomer[e]	β^A chain	oxygenated	-22.4 ± 0.3
tetramer ↔ monomer[e]	β^A chain	deoxygenated	-19 ± 0.3
dimer ↔ monomer[f]	α^A chain	oxygenated and deoxygenated	-5.3 ± 0.1

[a] This work: 50 mM Bis-Tris, 0.1 M NaCl, 1 mM Na_2EDTA, and 0.1 mM KCN, pH 7.3 and 21 °C. [b] Data from Mrabet et al. (*71*): 10 mM sodium phosphate, pH 7.0 and 25 °C. [c] Data from Turner et al. (*9*): 0.1 M Tris 0.1 M NaCl, and 1 mM Na_2EDTA, pH 7.4 and 21.5 °C. [d] Philo et al. (*27*): 0.1 M Tris-HCl, 0.1 M NaCl, and 1 mM EDTA, pH 7.4 and 15 °C. [e] Valdes and Ackers (*1*): same experimental conditions as ref *9*. [f] Valdes and Ackers (*26*): same experimental conditions as ref *9*.

Subunit Assembly by Gel Filtration. The subunit assembly of cyanometHb derivatives was measured by gel filtration on Superose 12 with an HPLC system. Small zone profiles were analyzed to determine the subunit association versus the protein concentration (*49*, *50*). This procedure differs from the experiments based on the large zone profiles where the elution volumes of self-associating proteins are determined from the centroid positions of the trailing and leading edges (*26*). Although the dilution factor during elution is small in our experiments, it remains a significant factor. Consequently, the free energies of subunit assembly ($\Delta G_{assembly}$) measured by gel filtration on Superose 12 might be overestimated by a few tenths of kilocalories per mole. For this reason, we measured the $\Delta G_{assembly}$ of the cyanometHb A system, which has been extensively studied with large zone gel filtration by Ackers and his collaborators. We found a dimer−tetramer assembly free energy equal to -8.9 ± 0.1 kcal/mol (Table 2) in our standard conditions (0.05 mM Bis-Tris, 0.1 M NaCl, 1 mM Na_2EDTA, and 0.1 mM KCN, pH 7.3, at 21 °C), whereas Huang et al. (*51*) reported a value of -9.0 ± 0.2 kcal/mol in similar experimental conditions (0.1 M Tris, 0.08 M NaCl, 1 mM Na_2EDTA, and 0.01 mM KCN, pH 7.4, at 21.5 °C). This agreement allowed us to validate the measurement of subunit assembly employing the Superose 12 gel filtration procedure, in agreement with the results of Manning et al. (*49*).

The elution profile of Ψ Hb at 50 μM (heme) is shown in Figure 4, in comparison with the elution profiles of Hb A tetramers, dimers, and monomers. At this concentration the

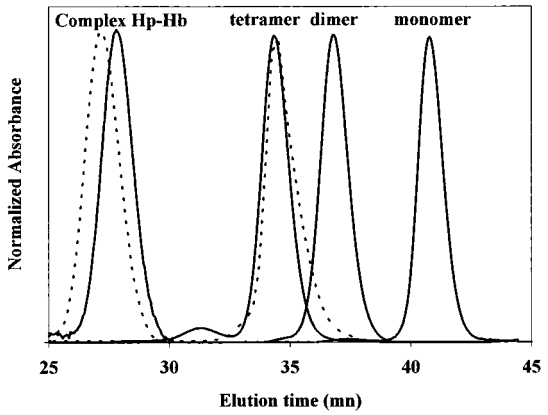

FIGURE 4: Elution profiles measured by gel chromatography on Superose 12. The solid lines are the references for Hb monomer, dimer, and tetramer and a covalent complex formed between a Hb dimer and a Hp dimer. The profile of Ψ Hb at 50 μM heme concentration (right dotted line) shows that the protein is essentially tetrameric. As observed for Hb A, two Ψ globins are bound per Hp dimer (left dotted line).

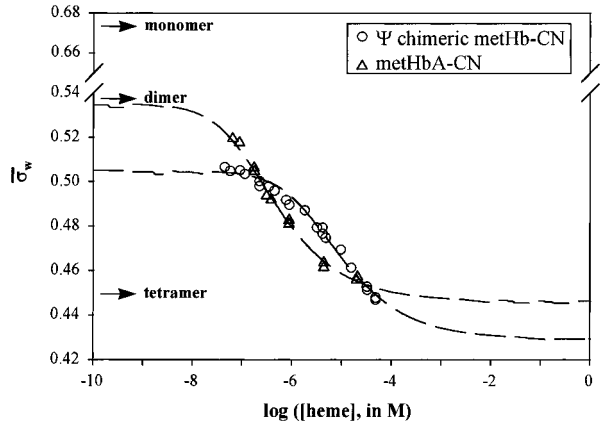

FIGURE 5: CyanometHb dimer−tetramer association of Hb A and Ψ Hb measured by gel chromatography on Superose 12. Weight average coefficients ($\overline{\sigma_w}$) are plotted as a function of the logarithm of heme concentration.

chimeric protein is essentially present in the tetrameric form. We studied the effect of the protein concentration on subunit self-association. The experiments were performed with the cyanometHb form, which is structurally similar to the fully oxygenated Hb tetramer. Indeed, the autoxidation of oxy Hb is a limiting factor in the study of subunit association by gel filtration especially at low protein concentration because of the fast rate of autoxidation for Hb dimers (*52*); a non-negligible fraction of metHb might change the subunit association equilibrium of an oxy Hb solution. The weight-average partition coefficients ($\overline{\sigma_w}$) for Hb A and Ψ Hb cyanomet derivatives as a function of the logarithm of the total protein concentration are shown in Figure 5. The isotherms were simulated with a dimer−tetramer equilibrium model in the range of protein concentration investigated. Different dimer and tetramer end points were found for Hb A and Hb Ψ. This discrepancy may be due at least in part to a different hydration of both proteins. Indeed, protein elution on gel filtration is not strictly correlated with the protein molecular mass but also with its geometry and, more generally, with its Stoke radius (*53*). The Ψ tetramer possesses only 10 amino acids more than the Hb A tetramer (2% of the amino acid content), but these amino acids are involved in the formation of the two α helices lacking in the α globins. Different weight partition coefficients corresponding to the monomer end points were estimated by large zone gel filtration of α and β chains (*26*).

A number of observations are consistent with a dimer−tetramer equilibrium of Ψ Hb with a dissociation constant in the micromolar range. First, chimeric Hb, as described below under O_2 Binding at Equilibrium, binds to an allosteric effector which interacts only with a specific site of the Hb tetrameric structure. Second, the chimeric Hb forms a complex with Hp which is known to trap the Hb dimers. The Hp binds two Hb dimers for a total molecular mass of 150 kDa. The Hp−Hb binding was observed by gel filtration since the molecular mass of the complex is approximately 2-fold higher than those of Hb and Hp, 65 kDa and 85 kDa, respectively. Figure 4 shows the elution profiles of Hp−Hb complexes for Hb A and Ψ Hb detected in the visible domain where Hp does not absorb. No attempt was made to characterize the mechanism of protein−protein interaction between Hp and Ψ Hb, but the binding of two Hb dimers (1 μM total concentration) by an excess of only two Hp dimers suggests that this interaction is specific and occurs with a high affinity. The lower elution volume observed for Hp−Ψ Hb compared with Hp−Hb A matches well with the lower partition coefficient of the chimeric dimer (Figure 5). Nagel and Gibson (*54*) have reported that Hp binds four α chains but not β chains. We confirmed by gel filtration that 1 equiv of α chain is totally bound to a 2-fold equivalent of Hp, but we also observed a partial interaction between the β chains and Hp (data not shown). Then Hp might interact either with Ψ Hb dimers or with monomers for a total of four chimeric globins per Hp molecule. We found that the dimer−tetramer model provided an excellent fit of our subunit association data. However, we cannot eliminate the possibility of a small amount of higher aggregation states especially in the region covering the end points. The dimer−tetramer interface of Ψ Hb was estimated to be 2 kcal/mol less favorable than the allosteric interface $\alpha_1\beta_2$ of cyanometHb A (only 1 kcal/mol compared to oxy Hb A; Table 2). It was not possible to measure the free energy of monomer−dimer assembly Ψ Hb by gel filtration using a light detection mode. We assumed that this interface is very stable, as is the $\alpha_1\beta_1$ interface of Hb A, and that the free energy for the interface formation is less than −10 kcal/mol of monomer.

Autoxidation Kinetics. A crucial role of the globin structure is to protect the iron against autoxidation. Free heme in solution is oxidized on contact with dissolved oxygen (milliseconds), while within the heme pocket of Hb A the autoxidation rate is 10^6-fold slower. The autoxidation is correlated with the O_2 affinity since the main natural oxidant of the iron is precisely the O_2 molecule (*55*). Because the O_2 affinity is directly proportional to the O_2 dissociation rate, the O_2 dissociation frequency will affect both the O_2 affinity and the frequency for the transfer of an electron from ferrous iron to an O_2 molecule to give rise to a superoxide anion. Once the iron is oxidized, it does not bind O_2, and the superoxide anion is involved in several side reactions, such as its conversion into hydrogen peroxide, which further catalyzes Hb oxidation. The quaternary structure of Hb A also plays a significant role in the autoxidation process because of its influence on the structure

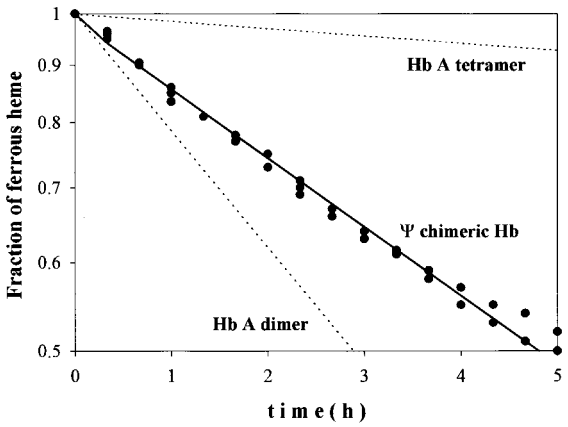

FIGURE 6: Kinetics of autoxidation of Ψ Hb, fully saturated under 1 atm of O_2. Experimental conditions were 50 mM Bis-Tris and 100 mM NaCl buffer, pH 7.0, at 37 °C. The autoxidation kinetics for Hb A dimers and tetramers are taken from Griffon et al. (*57*), where the experimental conditions were 20 mM sodium phosphate buffer, pH 7.0, at 37 °C.

of the heme pocket. The removal of the tertiary constraints applied by the Hb tetrameric structure on the heme pocket when tetramers dissociate into dimers induces a 17-fold increase of the rate of autoxidation (*52*). This result is not related to dimer and tetramer O_2 affinities under O_2 saturation conditions, since these affinities are similar. The exposure to the solvent of the buried $\alpha_1\beta_2$ interface and the loss of contacts between the C helix and the FG corners of both subunits are expected to change the heme pocket structure. A consequence is the increase of the rate constant for hemin dissociation from dimers compared to tetramers (*56*). At 37 °C and pH 7.0, the autoxidation rates for Hb tetramers and dimers were 0.015 and 0.24 h^{-1}, respectively (Figure 6; 57). We measured the autoxidation of Ψ Hb at various protein concentrations to test the difference in oxidation between dimers and tetramers. In the range of concentration studied the dimer fraction should change from 60% to 90%, taking the dimer−tetramer equilibrium constant estimated by gel filtration. No detectable variation of autoxidation was found versus the Ψ Hb concentration, and the rate of oxidation was calculated with a global fit of the data set (Figure 6). The absence of a difference between the dimer and tetramer rates of oxidation might be due to a compensation between the relative stabilities of both structures and their O_2 affinities; the chimeric dimers could be less stable than the tetramer, but their O_2 affinity is 6-fold higher. The rate of autoxidation for a Ψ tetramer was around 2-fold lower than that of a Hb dimer (0.14 h^{-1}). This rate seems to follow the relation between oxidation and O_2 affinity, including the comparison of noncooperative Mb. In similar experimental conditions (+EDTA) the rate of oxidation for sperm whale Mb is equal to 0.055 h^{-1} (*55*) with an O_2 affinity 7-fold higher than for the chimeric Hb tetramer (Table 3).

O_2 and CO Association and Dissociation Kinetics. Once the CO is photodissociated, it can rebind via two different pathways: (i) the nanosecond geminate phase for the ligands which have not diffused away from the heme and (ii) the millisecond bimolecular phase in which the ligand released from the protein matrix comes from the solvent. The fraction of the bimolecular phase increases for higher temperature, lower solvent viscosity, and proteins with slower on-rates (*58*). CO bimolecular kinetics of Ψ Hb after flash photolysis are shown in Figure 7. At 25 °C the CO bimolecular fraction for Ψ Hb was about 80% instead of 55% for Hb A in the R-state and 98% for Mb (*59*). This result can be explained if we assume that the main energetic potential which governs the CO binding is modulated by the association rates rather than the escape rates. The CO association rates for Ψ Hb are intermediate between those of R-state Hb A and Mb (Table 3).

Two distinct bimolecular phases were observed for Ψ Hb, and their relative amplitudes were found to be dependent on protein concentration. The fast phase was predominant at low protein concentration, whereas the slow phase was predominant at high protein concentration. We attributed the fast component to the dimer fraction and the slow component to the tetramer fraction (Figure 7).

Typically, HbCO bimolecular kinetics exhibit a biphasic pattern. The fast phase is associated with the CO rebinding characteristic of a R-state Hb that comprises mainly the triliganded species, and the slow phase is associated to the deoxy T-state species. The slow phase contribution increases with the CO dissociation level because the fully deoxy and monoliganded species are more populated. The variation of CO rebinding kinetics with respect to the laser photodissociation level is a practical marker of Hb cooperativity behavior upon ligand association and release. The CO rebinding kinetics of β/α chimera Hb did not show cooperative behavior. The two bimolecular phases of Ψ Hb depend only on the subunit aggregation state. The value of $^4K_2$ determined by the protein concentration dependence of CO rebinding was in agreement with the value determined by gel filtration. The dimer CO association rate of Ψ Hb is 4 times faster than that of tetramer. This contrasts with "quaternary enhancement" mentioned for the homotetramer β_4 since the CO association rate of a β monomer is slower than for a homotetramer (Table 3; ref *27*) but corresponds more closely to the Hb A mechanism whereby "quaternary constraint" lowers the ligand affinity of the Hb A tetramer. It should be noted that the functional inequivalence of the α and β chains in the Hb R-state is very slight under our experimental conditions ($\leq$0.2 kcal/mol). We found that the β chains are faster than the α chains for both CO binding ($\approx$2-fold) and CO release ($\approx$3-fold).

From these kinetic studies we conclude that the CO affinity of Ψ Hb is intermediate between Hb R- and T-states (Table 3). The increase of O_2 dissociation velocity that follows the dimer aggregation into tetramer is shown in the inset of Figure 7, whereas no change in the O_2 on-rates was found. The O_2 off-rate is 6-fold faster for a chimeric tetramer in comparison with a dimer, thereby lowering the intrinsic O_2 affinity of the tetramer.

O_2 Binding at Equilibrium. We measured the O_2 binding isotherms for Ψ Hb and Hb A. As shown in Figure 8, Ψ Hb does not exhibit cooperativity of O_2 binding, with a Hill slope equal to 1 over the entire range of saturation, whereas the maximum slope was 2.8 for Hb A. Mills et al. (*2*) found a slightly higher Hill coefficient (n_{max} = 3.3) for a pure tetramer isotherm simulated with a study of the protein concentration dependence of oxygenation curves. Since the dimer and tetramer fractions were almost equally populated at 12 μM heme concentration, the O_2 isotherm comprises the dimer and tetramer oxygen binding properties (Figure

Table 3: CO and O_2 Binding Properties of Ψ Chimeric Hb[a]

species	$k_{on}^{CO} \times 10^{-6}$ (M^{-1} s^{-1})	k_{off}^{CO} (s^{-1})	$K^{CO} \times 10^{7}$ (M)	$k_{on}^{O_2} \times 10^{-6}$ (M^{-1} s^{-1})	$k_{off}^{O_2}$ (s^{-1})	$K^{O_2} \times 10^{5}$ (M)	partition coefficient, K^{O_2}/K^{CO}
Ψ Hb dimer	8.0	0.036	0.04	40	50	0.12	300
Ψ Hb tetramer	2.2	0.036	0.16	36	300	0.83	500
Ψ Hb +RSR4	4.0						
	0.9			26.3	330	1.26	
human Hb A (R)[e]	10.5	0.022	0.021	73.5	64	0.09	400
	4.5	0.008	0.018	32.0	40	0.12	700
human Hb A (T)	0.17 (+RSR4)	0.1[d]	5.9	4.1 (+RSR4)	1800[b]	44	800
α monomer	4.5	0.013[c]	0.029	35.5	40.6	0.11	400
β tetramer	12.2	0.008[c]	0.006	63.2	27.9	0.04	700
β monomer	4.7	0.008[c]	0.017	63.2			
horse Mb	0.5	0.017[c]	0.34	19.7	21.6	0.11	30

[a] In this work, experimental conditions were 50 mM Bis-Tris, 0.1 M NaCl, and 1 mM Na_2EDTA (±0.5 mM RSR4), 25 °C and pH 7.2. Typical standard deviations were between 5% and 15%. [b] From Kiger et al. (*59*); value for β subunits: 50 mM Bis-Tris, 0.1 M NaCl, and 0.5 mM IHP, 25 °C and pH 6.6. [c] From Antonini and Brunori (*39*): 0.1 M potassium phosphate, 20 °C and pH 7.0. [d] From Samaja et al. (*72*); value for β subunits: 0.02 mM potassium phosphate, 50 mM KCl, and 1 mM EDTA, 20 °C and pH 7.0. [e] The fast and slow phases were attributed to β the α and chains from the work of Olson et al. (*73*).

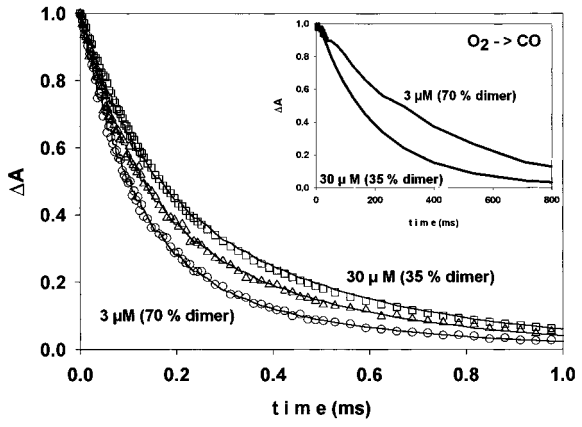

FIGURE 7: CO bimolecular kinetics of Ψ Hb at 3, 10, and 30 μM protein concentrations (heme basis). The CO association velocity for chimeric subunits was slower for a tetramer compared to a dimer. The fraction photodissociated was 80% at 25 °C and was normalized to the maximum absorbance change which occurred at the highest temperature (45 °C). In the inset is shown the O_2 replacement by CO after flash photolysis. The phase of replacement is faster for the chimeric tetramers due to a higher O_2 dissociation rate compared to the chimeric dimers. The experimental conditions are described in Materials and Methods.

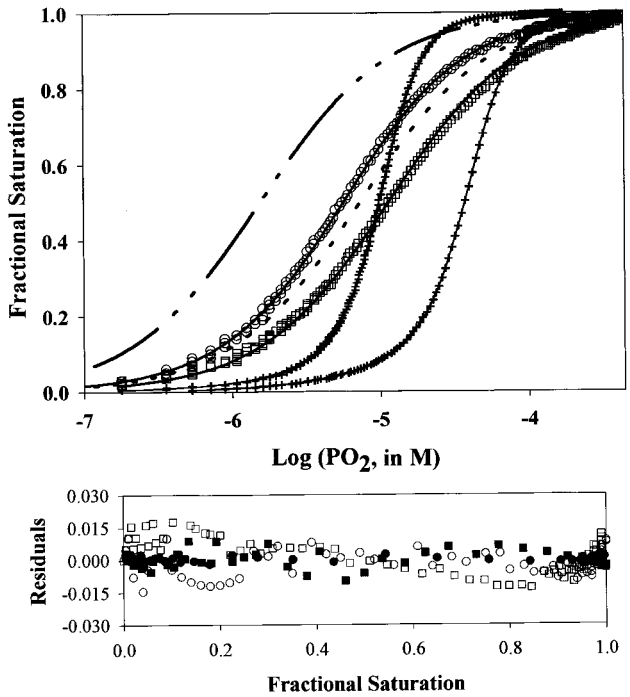

FIGURE 8: Oxygenation isotherms of Ψ Hb at 12 μM heme concentration with (squares) and without RSR4 (circles), a potent allosteric effector. The theoretical curves for O_2 binding to pure Ψ dimer and tetramer forms are shown as double-dot−dashed and dotted lines, respectively. These isotherms are generated with the partition function described in Material and Methods. Since we did not measure the dimer−tetramer assembly equilibrium constant of Ψ Hb with RSR4, the O_2 isotherm is simulated with a single binding constant in the absence of cooperativity behavior. Oxygenation isotherms of Hb A are also given for comparison as cross symbols, with (right shifted) and without RSR4 (left shifted).

8). The simulations of the O_2 binding curves were obtained using the intrinsic O_2 affinities for chimeric dimers and tetramers estimated with O_2/CO replacement kinetics and assuming identical stepwise binding constants for the tetramer. This last assumption is obviously valid since no cooperativity or anticooperativity was detected during the deoxygenation reaction. It should be emphasized that direct calculations of pure dimer and tetramer O_2 binding isotherms from the O_2 equilibrium studies are difficult. Indeed, by varying the protein concentration within the limits of detection of our method, the shift of P_{med} will be less than to 0.5 mmHg. The dimer O_2 binding free energy (−8 kcal/mol of O_2) is 1 kcal/mol more favorable than that of a tetramer, and consequently, as for Hb A, the O_2 isotherm of the Ψ tetramer lies to the right of that of the dimer (Figure 8). The linkage scheme between the subunit association and the stepwise O_2 binding predicts a 4 kcal/mol more stable tetramer after the O_2 release (Figure 9).

Effector Binding. The heterotropic effects of Ψ Hb were measured after the addition of RSR4, a potent allosteric effector of Hb A (*40*). There are two symmetrical binding sites for RSR4 located in the central cavity of HbA. Three major contacts between protein amino acids and RSR4 have been determined by X-ray crystal studies that involve Lys α_1 (G6) 99, Arg α_2 (HC3) 141, and Asn β_1 (G10) 108 (*40*). The RSR4 binding to Hb A induces a shift of the allosteric equilibrium toward the low-affinity T-state and a decrease

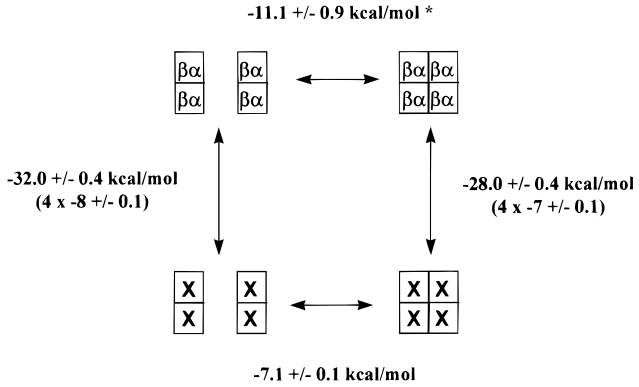

FIGURE 9: Linkage scheme for oxygenation and assembly of Ψ Hb. The dimer−tetramer assembly free energy of deoxy Ψ Hb (*) is determined from the conservation free energy around the linkage scheme.

of the R and T intrinsic oxygen affinities (*60*). Both α residues are conserved in the globin sequence of Ψ Hb, but Asn β G10 is replaced by a histidine residue which may stabilize the effector binding as well; the histidine side-chain amino group as a hydrogen donor is also susceptible to interacting with the π electrons of the aromatic rings of the RSR4 compound (*61*, *40*). The addition of RSR4 induced a right shift of the O_2 isotherm (toward higher O_2 partial pressures) for the chimeric Hb solution (Figure 8; Table 3). These heterotropic effects upon RSR4 binding probably lead to a shift of the dimer−tetramer equilibrium in favor of tetramers, coupled with a change of the intrinsic O_2 affinity of the tetramer. The CO association kinetics confirmed the slight decrease of ligand affinity after effector binding to the tetramer (Table 3). It is likely that this heterotropic ligand interacts with a specific protein site of the Ψ tetramer rather than the Ψ Hb dimer since allosteric effectors such as RSR4 tie down three subunits to effect their action on Hb A (α_1, α_2, β_1). An interaction between a Ψ Hb dimer and RSR4 would imply a nonspecific binding. Interestingly, no heterotropic effect of RSR4 was observed with the isolated β and α chains or with sperm whale Mb. The absence of heterotropic effects with 2,3-DPG or IHP on the Ψ Hb tetramers is indicative of alterations at the binding site of organophosphates. Two key residues of the 2,3-DPG site, Lys β (EF6) 82 and His β (H21)143, located between the β chains in the central cavity of Hb A (*62*), are absent in the Ψ globin structure.

DISCUSSION

The Ψ globin is composed of 146 amino acids that in Hb form eight connected α helices: the first five α helices of a β chain followed by the last three α helices of an α chain. As shown in Table 2, the subunit aggregation of α chains, β chains, and $(\alpha\beta)_2$ tetramers proceeds by different mechanisms according to the relative stability of the subunit interfaces. The chimeric Ψ globin assembly in solution resembles that of HbA based on the two successive equilibria:

$$4\ \Psi \text{ monomers} \rightleftharpoons 2\ \Psi \text{ dimers} \rightleftharpoons \Psi \text{ tetramer}$$

The result of the subunit assembly into a tetramer is the formation of two distinguishable interfaces, intra- and interdimer. Interestingly, the intradimer interface is much more stable than those of α and β isolated chains (Table 2). This is comparable to what is observed in oxy Hb A where the most stable contacts between the subunits occur at the intradimer interfaces $\alpha_1\beta_1$ (or $\alpha_2\beta_2$). The analysis of the hydropathic interactions of these interfaces in Hb A, using the HINT program based on experimentally determined hydropathy values of thousands of organic molecules, showed that they are essentially stabilized via several favorable polar and hydrophobic interactions in both R and T structures (*8*). Another common feature between the chimeric tetramer and Hb A is the stabilization of the interdimer interface in the deoxy state. This is in contrast to the deoxy homotetramer β_4, which is more dissociated toward the monomeric form (*1*). The cooperative mechanism in Hb A implies a stabilization of the interdimer interface, the allosteric interface $\alpha_1\beta_2$, after each ligand removal but to a different extent for the four ligand binding steps, as opposed to the chimeric Hb (Figure 9).

The intrinsic O_2 affinity is mediated by the O_2 off-rate, which is intermediate to the Hb A R- and T-state off-rates. The deoxy spectrum of the chimeric tetramer indicates a conformation of the heme that resembles that of an α chain. This suggests that the deoxy globin does not display the constraints present in deoxy Hb A which arise from the positions of the proximal F and G helices. As a result, the Fe−His (F8) bond of the Ψ globin is shortened, and the doming of the heme should be less pronounced. The faster O_2 dissociation rates of the chimeric Hb compared to the Hb A R off-rate might be due rather to some electronic effects on the Fe−O_2 bond of the heme or to distal effects of the heme pocket such as weaker interactions between the dipolar $Fe^{\delta+}-O-O^{\delta-}$ and the polar residues.

For the RSR compound family, the molecular bases of the effector intrinsic activity originate from the subtle interactions between the drug and three main residues of Hb A (Lys α_1 99, Arg α_2 141, and Asn β_1 108). Since these residues involve both α chains and a β chain, the property of Ψ Hb to bind the allosteric effector RSR4 is strong evidence for the formation of a tetrameric structure. This quaternary structure should be close to the native T structure of Hb A because allosteric effectors do not bind specifically to the oxy Hb R structure (*63*). The O_2 binding to deoxy Ψ tetramers could give rise to a perturbed structure that accounts for a less stable dimer−tetramer interface in the liganded state by the equivalent of 4 kcal/mol (2/3 of the cooperative free energy of Hb A). However, the absence of heme−heme interaction could also be explained by small structural changes during the oxygenation reaction. The formation of two hydrogen bonds as well as few van der Waals contacts is enough to account for 4 cal/mol.

Hb Ypsilanti, a natural variant of the Hb A dimer−tetramer interface, exhibits a similar mechanism for O_2 binding in that the cooperativity index is extremely low (Hill $n_{max} \cong 1.1$) and the cooperative free energy is reduced to 2.6 kcal/mol, but the intrinsic O_2 affinity for the mutant tetramer is higher than for the mutant dimer (*64*). The crystallographic studies of the carbonmonoxy form of Hb Ypsilanti showed a new quaternary structure Y or R2 (*65*). This structure is another liganded conformation, different from the R conformation (*66*). Similarly, the quaternary structure of Ψ Hb could be slightly different from that of the Hb A R and T conformations, although it could be closer to the low-affinity

end state due to Ψ Hb's interaction with RSR4. Since the chimeric Hb is not cooperative, the effect of RSR4 on oxygen binding is due to some influence on the heme pocket, which is probably related to the interaction of one of the chlorines inserted in a groove of the α G helix near Lys 99 (*60*). Phe α 98 and Leu α 100 flank the heme. This effector binding acts only on the intrinsic O_2 affinity of Ψ Hb, whereas its binding to Hb A acts on both the intrinsic O_2 affinity and the allosteric equilibrium.

The work reported here was carried out with a view to engineer a recombinant homotetramer that could serve as a potential blood substitute. Our work provides a proof of principle that it is possible to produce a stable recombinant homotetramer with an O_2 affinity (P_{50}) similar to that of Hb A. The oxygen delivery efficiency for an oxygen carrier in vivo depends in a simple way on the position and shape of its oxygen binding curve between the partial oxygen pressures at the lungs and at the tissues. The oxygen binding properties of the circulating erythrocytes are affected by numerous heterotropic ligands such as 2,3-DPG, chloride, CO_2, and H^+ (Bohr effect). As a result, the overall O_2 affinity is decreased by a factor of 2−3, allowing delivery of about 25% of oxygen molecules. For a cell-free solution of Hb A the oxygen delivery would be only 5% mainly due to the higher affinity (in the absence of 2,3-DPG) in comparison with at least 10% for a noncooperative molecule with an oxygen affinity such as that for the Ψ Hb (see Figure 3 from ref *67*). On the basis of the oxygen delivery estimations, the Ψ Hb would be more efficient than unmodified Hb A or β_4 solutions, but not sufficient to compete with a red cell suspension. To optimize the O_2 release between the physiological O_2 partial pressures, the O_2 affinity should be centered between these two limits. The absence of cooperativity is not necessarily a major handicap. While cooperativity may initially enhance the O_2 delivery to the tissues, the decrease in O_2 delivery due to methemoglobin formation is also enhanced, because oxidized subunits will also perturb the other subunits in the same tetramer (*68*). A ferric heme shifts the allosteric equilibrium by a factor of 30 toward the high O_2 affinity conformation, leading to a decrease of the cooperativity and an increase of the overall O_2 affinity. In contrast, oxidation of noncooperative subunits will not affect the remaining binding sites.

Another advantage of a homotetramer O_2 carrier is to avoid synthesizing matched amounts of both α and β genes. The expression of a heterotetramer $(\alpha\beta)_2$ with a satisfactory yield depends on the coordination of the synthesis of both genes. If one gene is overexpressed, the accumulation of that globin could induce a serious disruption of the host cell because of the instability of the excess α or β chains (*69*, *56*). Unfortunately, the expression system used did not produce a better yield in *E. coli* by comparison with a β A globin. The level of fusion protein for Ψ Hb was about 5−6% of the total soluble proteins of *E. coli* extract instead of 12% for a CIIFXβ^A protein.

One major, persistent problem inherent to all hemoglobin-based blood substitutes is the autoxidation rate of the hemes. This limits the useful lifetime of those O_2 carriers in vivo (*67*). It is also crucial to cross-link the tetramer to prevent renal filtration of the Hb dimers and their irreversible binding to haptoglobin. There are numerous Hb cross-linking reagents or other chemical compounds that have been described in the literature (*70*). A peptide link between subunits also can be engineered genetically to maintain the tetrameric form. A cross-linked Ψ homotetramer could be another step to estimate the potential of this new class of Hb-derived molecules as an O_2 carrier in vivo.

The Ψ globin is composed of the first 79 human β globin residues followed by the last 67 human α globin residues. The Ψ globin assembles into a stable tetramer and demonstrates that it is possible to engineer a functional recombinant Hb homotetramer with a moderate intrinsic O_2 affinity, intermediate between those of the R- and T-states of Hb A. The chimeric Hb mechanism differs from that of Hb by an absence of cooperativity of ligand binding. However, the quaternary restraints of the deoxy state in both proteins stabilize the interdimer interface in comparison with the liganded state (−4 kcal/mol of tetramer for Ψ Hb).

ACKNOWLEDGMENT

We thank Dr. O. Bertrand for helpful comments and for assistance in the gel filtration experiments and Pr. J. M. Manning for a critical reading of the manuscript. We thank Dr. V. Baudin, Dr. J. Kister, Dr. P. Genin, E. Domingues and G. Caron for their continuous support. We thank Dr. H. Wajcman and the Baxter Healthcare Company for providing Hb Rothschild and DCL Hb, respectively.

REFERENCES

1. Valdes, R., Jr., and Ackers, G. K. (1978) *Proc. Natl. Acad. Sci. U.S.A. 75*, 311−314.
2. Mills, F. C., Johnson, M. L., and Ackers, G. K. (1976) *Biochemistry 15*, 5350−5362.
3. Philo, J. S., and Lary, J. W. (1990) *J. Biol. Chem. 265*, 139−143.
4. Gibson, Q. H., and Edelstein, S. J. (1987) *J. Biol. Chem. 262*, 516−519.
5. Edelstein, S. J. (1975) *Annu. Rev. Biochem. 44*, 209−232.
6. Baldwin, J., and Chothia, C. (1979) *J. Mol. Biol. 129*, 175−220.
7. Perutz, M. F. (1989) *Q. Rev. Biophys. 22*, 139−237.
8. Abraham, D. J., Kellogg, G. E., Holt, J. M., and Ackers, G. K. (1997) *J. Mol. Biol. 272*, 613−632.
9. Turner, G. J., Galacteros, F., Doyle, M. L., Hedlund, B., Pettigrew, D. W., Turner, B. W., Smith, F. R., Moo-Penn, W., Rucknagel, D. L., and Ackers, G. K. (1992) *Proteins 14*, 333−350.
10. Monod, J., Wyman, J., and Changeux, J. P. (1965) *J. Mol. Biol. 12*, 88−118.
11. Perrella, M., Davids, N., and Rossi-Bernardi, L. (1992) *J. Biol. Chem. 267*, 8744−8751.
12. Perrella, M., and Denisov, I. (1995) *Methods Enzymol. 259*, 468−487.
13. Edelstein, S. J. (1996) *J. Mol. Biol. 257*, 737−744.
14. Marden, M. C., Griffon, N., and Poyart, C. (1996) *J. Mol. Biol. 263*, 90−97.
15. Huang, Y., Doyle, M. L., and Ackers, G. K. (1996) *Biophys. J. 71*, 2094−2105.
16. Shibayama, N., Morimoto, H., and Saigo, S. (1997) *Biochemistry 36*, 4375−4381.
17. Ackers, G. K., Perrella, M., Holt, J. M., Denisov, I., and Huang, Y. (1997) *Biochemistry 36*, 10822−10829.
18. Pardon, E., Haezebrouck, P., De Baetselier, A., Hooke, S. D., Fancourt, K. T., Desmet, J., Dobson, C. M., Van Dael, H., and Joniau, M. (1995) *J. Biol. Chem. 270*, 10514−10524.
19. Lijnen, H. R., Wnendt, S., Schneider, J., Janocha, E., Van Hoef, B., Collen, D., and Steffens, G. J. (1995) *Eur. J. Biochem. 234*, 350−357.
20. Quinn, G. B., Trimboli, A. J., and Barber, M. J. (1994) *J. Biol. Chem. 269*, 13375−13381.

21. Picard, D. (1994) *Curr. Opin. Biotechnol. 5*, 511−515.
22. Rao, M. J., Manjula, B. N., Kumar, R., and Acharya, A. S. (1996) *Protein Sci. 5*, 956−965.
23. Bunn, H. F., and Forget, B. G. (1986) In *Hemoglobin: Molecular, Genetic and Clinical Aspects*, pp 416−417, W. B. Saunders Co., Philadelphia.
24. Dumoulin, A., Baudin, V., Kiger, L., Edelstein, S. J., Marden, M., Poyart, C., and Pagnier, J. (1994) *Artif. Cells, Blood Substitutes, Immobilization Biotechnol. 22*, 733−738.
25. Schaad, O., Vallone, B., and Edelstein, S. J. (1993) *C. R. Acad. Sci. Ser. III 316*, 564−571.
26. Valdes, R., Jr., and Ackers, G. K. (1977) *J. Biol. Chem. 252*, 74−81.
27. Philo, J. S., Lary, J. W., and Schuster, T. M. (1988) *J. Biol. Chem. 263*, 682−689.
28. Komiyama, N. H., Shih, D. T., Looker, D., Tame, J., and Nagai, K. (1991) *Nature 352*, 349−351.
29. Bihoreau, M. T., Baudin, V., Marden, M., Lacaze, N., Bohn, B., Kister, J., Schaad, O., Dumoulin, A., Edelstein, S. J., and Poyart, C. (1992) *Protein Sci. 1*, 145−150.
30. Nagai, K., and Thogersen, H. C. (1984) *Nature 309*, 810−812.
31. Winterhalter, K. H., and Colosimo, A. (1971) *Biochemistry 10*, 621−624.
32. Bucci, E., and Fronticelli, C. (1965) *J. Biol. Chem. 240*, 551−553.
33. Vandegriff, K. D., Le Tellier, Y. C., Winslow, R. M., Rohlfs, R. J., and Olson, J. S. (1991) *J. Biol. Chem. 266*, 17049−17059.
34. Hayashi, A., Suzuki, T., and Shin, M. (1973) *Biochim. Biophys. Acta 310*, 309−316.
35. Van Assendelft, O. W. (1970) In *Spectrophotometry of haemoglobin derivatives*, p 72, Royal Vangorcum Ldt., Assen, The Netherlands.
36. Ziljstra, W. G., and Buursma, A. (1987) *Comp. Biochem. Physiol. 88B*, 251−255.
37. Kister, J., Poyart, C., and Edelstein, S. J. (1987) *J. Biol. Chem. 262*, 12085−12091.
38. Wyman, J., and Gill, S. J. (1990) in *Binding and linkage*, pp 221−227, University Science, Mill Valley, CA.
39. Antonini, E., and Brunori, M. (1971) In *Hemoglobin and myoglobin in their reactions with ligands*, pp 120−122, 197−198, 226, and 310, North-Holland Publishing Co., Amsterdam.
40. Abraham, D. J., Wireko, F. C., Randad, R. S., Poyart, C., Kister, J., Bohn, B., Liard, J. F., and Kunert, M. P. (1992) *Biochemistry 31*, 9141−9149.
41. Fenn, J. B., Mann, M., Meng, C. K., Wong, S. F., and Whitehouse, C. M. (1989) *Science 246*, 64−71.
42. Weber, G., and Teale, F. J. W. (1959) *Discuss. Faraday Soc. 27*, 134−139.
43. Marden, M. C., Hui Bon Hoa, G., and Stetzkowski-Marden, F. (1986) *Biophys. J. 49*, 619−627.
44. Perutz, M. F., Ladner, J. E., Simon, S. R., and Ho, C. (1974) *Biochemistry 13*, 2163−2173.
45. Perutz, M. F., Fermi G., Abraham, D. J., Poyart, C., and Burseaux, E. (1986) *J. Am. Chem. Soc. 108*, 1064−1078.
46. Olson, J. S. (1976) *Proc. Natl. Acad. Sci. U.S.A. 73*, 1140−1144.
47. Eaton, W. A., Hanson, L. K., Stephens, P. J., Sutherland, J. C., and Dunn, J. B. R. (1978) *J. Am. Chem. Soc. 100*, 4991−5003.
48. Kiger, L., Stetzkowski-Marden, F., Poyart, C., and Marden, M. C. (1995) *Eur. J. Biochem. 228*, 665−668.
49. Manning, L. R., Jenkins, W. T., Hess, J. R., Vandegriff, K., Winslow, R. M., and Manning, J. M. (1996) *Protein Sci. 5*, 775−781.
50. Gallagher, C. N., and Huber, R. E. (1997) *Biochemistry 36*, 1281−1286.
51. Huang, Y., Koestner, M. L., and Ackers, G. K. (1996) *Biophys. J. 71*, 2106−2116.
52. Zhang, L., Levy, A., and Rifkind, J. M. (1991) *J. Biol. Chem. 266*, 24698−24701.
53. Ackers, G. K. (1975) In *The proteins* (Neurath, H., and Hill, R. L., Eds.) p 1, Academic Press, New York.
54. Nagel, R. L., and Gibson, Q. H. (1967) *J. Biol. Chem. 242*, 3428−3434.
55. Brantley, R. E., Jr., Smerdon, S. J., Wilkinson, A. J., Singleton, E. W., and Olson, J. S. (1993) *J. Biol. Chem. 268*, 6995−7010.
56. Hargrove, M. S., Whitaker, T., Olson, J. S., Vali, R. J., and Mathews, A. J. (1997) *J. Biol. Chem. 272*, 17385−17389.
57. Griffon, N., Baudin, V., Dieryck, W., Dumoulin, A., Pagnier, J., Poyart, C., and Marden, M. C. (1998) *Protein Sci.* (in press).
58. Beece, D., Eisenstein, L., Frauenfelder, H., and Gunsalus, I. C. (1980) *Biochemistry 19*, 5147−5157.
59. Kiger, L., Poyart, C., and Marden, M. C. (1993) *Biophys. J. 65*, 1050−1058.
60. Abraham, D. J., Kister, J., Joshi, G. S., Marden, M. C., and Poyart, C. (1995) *J. Mol. Biol. 248*, 845−855.
61. Levitt, M., and Perutz, M. F. (1988) *J. Mol. Biol. 201*, 751−754.
62. Arnone, A. (1972) *Nature 237*, 146−149.
63. Mehanna, A. S., and Abraham, D. J. (1990) *Biochemistry 29*, 3944−3952.
64. Doyle, M. L., Lew, G., Turner, G. J., Rucknagel, D., and Ackers, G. K. (1992) *Proteins 14*, 351−362.
65. Smith, F. R., Lattman, E. E., and Carter, C. W. (1991) *Proteins 10*, 81−91.
66. Schumacher, M. A., Zheleznova, E. E., Poundstone, K. S., Kluger, R., Jones, R. T., and Brennan, R. G. (1997) *Proc. Natl. Acad. Sci. U.S.A. 94*, 7841−7844.
67. Marden, M. C., Griffon, N., and Poyart, C. (1995) *Transfus. Clin. Biol. 2*, 473−480.
68. Marden, M. C., Kiger, L., Kister, J., Bohn, B., and Poyart, C. (1991) *Biophys. J. 60*, 770−776.
69. Sanna, M. T., Razynska, A., Karavitis, M., Koley, A. P., Friedman, F. K., Russu, I. M., Brinigar, W. S., and Fronticelli, C. (1997) *J. Biol. Chem. 272*, 3478−3486.
70. Sanders, K. E., Ackers, G., and Sligar, S. (1996) *Curr. Opin. Struct. Biol. 6*, 534−540.
71. Mrabet, N. T., Shaeffer, J. R., McDonald, M. J., and Bunn, H. F. (1986) *J. Biol. Chem. 261*, 1111−1115.
72. Samaja, M., Rovida, E., Perrella, M., and Rossi-Bernardi, L. (1987) *J. Biol. Chem. 262*, 4528−4533.
73. Olson, J. S., Mathews, A. J., Rohlfs, R. J., Springer, B. A., Egeberg, K. D., Sligar, S. G., Tame, J., Renaud, J. P., and Nagai, K. (1988) *Nature 336*, 265−266.

BI972689Z